

## Polymerization of substituted acetylenes and features of the formed polymers

Masashi Shiotsuki,<sup>\*a</sup> Fumio Sanda<sup>a</sup> and Toshio Masuda<sup>b</sup>

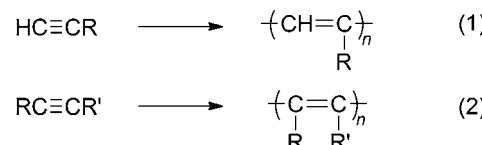
Received 5th October 2010, Accepted 17th November 2010

DOI: 10.1039/c0py00333f

Progress in the polymerization of substituted acetylenes and the properties and functions of the formed polymers that have been synthesized in the past several years are surveyed. Polymerization catalysts for substituted acetylenes, new monomers and polymers, controlled polymerizations, and photoelectronic functions and separation membranes of substituted polyacetylenes are discussed. A focus is placed on the development of novel rhodium catalysts for the polymerization of phenylacetylenes, the helical structures of the polymers obtained from chiral monosubstituted acetylenes, and highly gas-permeable polymers prepared from disubstituted acetylenes, in which great advances have been made recently.

### 1 Introduction

Substituted acetylenes, which are typically mono- or disubstituted, can be polymerized by chain growth in the presence of suitable transition metal catalysts to yield high molecular weight polymers (eqn (1) and (2)). The mono- and disubstituted acetylenes are classified as aliphatic or aromatic and then further categorized as hydrocarbon-based or heteroatom-containing monomers. The polymers possess carbon–carbon alternating double bonds along the main chain, in which the extent of the conjugation depends on the number, type, and bulkiness of the side groups.

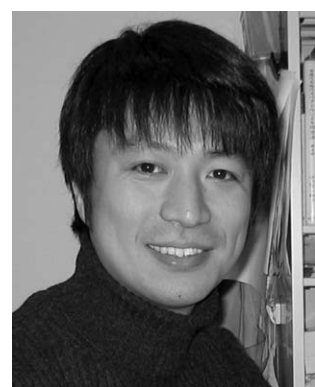


(R, R': alkyl, aryl, functional group)

Transition metals of various groups in the periodic table, including Nb, Ta, Mo, W, Fe, Ru, Rh, and Pd, are effective in the polymerization of substituted acetylenes. The types of monomers that are polymerizable with a particular catalyst are rather restricted; hence, it is important to recognize the characteristics of each catalyst. Two types of reaction mechanisms may be involved, depending on the polymerization catalysts used. One is the metathesis mechanism, whereby the active species are metal carbenes, namely, species having a metal–carbon double bond and the other is the insertion mechanism in which the active species are alkyl metals, namely, species having a metal–carbon single bond. These mechanisms can be distinguished from each other according to the catalysts used but are rather difficult to

<sup>a</sup>Department of Polymer Chemistry, Graduate School of Engineering, Kyoto University Katsura Campus, Kyoto, 615-8510, Japan. E-mail: shiotsuki@adv.polym.kyoto-u.ac.jp

<sup>b</sup>Department of Environmental and Biological Chemistry, Faculty of Engineering, Fukui University of Technology, 3-6-1 Gakuen, Fukui, 910-8505, Japan



Masashi Shiotsuki

Masashi Shiotsuki has been an Assistant Professor at the Graduate School of Engineering at Kyoto University since 2003. He received his DEng degree in 2003 from the Graduate School of Engineering at Kyoto University under the supervision of Professor Take-aki Mitsudo. His research interests include transition metal-catalyzed polymerization and conjugated polymers, including substituted polyacetylenes.



Fumio Sanda

Fumio Sanda is currently an Associate Professor at Kyoto University. His research interests include amino acid based polymers, optically active conjugated polymers, and precisely controlled polymerization. He is an Editor of Polymer Reviews and Journal of the Adhesion Society of Japan.

distinguish based on the polymer structure. Recently, the controlled polymerizations of phenylacetylene (PA), including living polymerization, have been intensively researched.

The carbon–carbon alternating double bonds in the main chain of these polymers can exhibit unique properties, including electrical conductivity, nonlinear optical properties, magnetic properties, gas permeability, and photo- and electroluminescent properties, which are not accessible from the corresponding vinyl polymers. The structure and properties of poly(phenylacetylene) [poly(PA)] have been studied in detail, particularly with respect to its geometric structure, helical structure, and photoluminescence. In contrast, disubstituted acetylene polymers are less conjugated due to steric hindrance, and so their photoelectronic functions have not been studied as much as those of monosubstituted acetylene polymers. Instead, disubstituted acetylene polymers are known as highly gas-permeable membrane materials due to their stiff main chain structure and the presence of spherical side groups.

This brief review surveys the polymerization of substituted acetylenes, focusing on the research performed over the past five years. Monomers and polymers, polymerization catalysts, controlled polymerizations, and functional polyacetylenes are discussed. Readers are encouraged to access other reviews and studies for a more comprehensive review of the polymerization of substituted acetylenes and the features of the substituted polyacetylenes that are formed.<sup>1–7</sup>

### 1.1 Recent advances in polymerization catalysts

In the early study of substituted polyacetylene chemistry, various transition metal catalysts were examined, but for the most part, early transition metal catalysts were found to be effective. In particular, metal halides such as  $\text{MoCl}_5$ ,  $\text{WCl}_6$ ,  $\text{TaCl}_5$ , and  $\text{NbCl}_5$  that are activated by alkylating agents successfully polymerize mono- and disubstituted acetylenes, resulting in high molecular weight polymers. In contrast, great efforts have been made in developing late transition metal catalysts in the past decade. Late transition metal catalysts complement early transition metal catalysts with respect to high tolerance towards air and moisture and the accessibility to well-defined catalysts suitable not only for living polymerization but also for the mechanistic studies of polymerization of substituted acetylenes. In this section, the late transition metal catalysts newly developed,



Toshio Masuda

*Toshio Masuda is currently a Professor at the Fukui University of Technology. His research interests include substituted polyacetylenes, transition metal catalyzed polymerization, gas separation membranes, and polymeric functional materials. He is an Associate Editor of Polymer.*

mainly since 2006, are discussed, along with some improvements of early transition metal catalysts.

**1.1.1 Rhodium catalysts.** Rh catalysts have been attracting much attention because of their high activity and the relatively wide range of applicable monomers that can produce functional polymer materials. Conventional Rh catalysts generally contain 2,5-norbornadiene (nbd) as a ligand. Representative catalysts (**1-nbd**, **2-nbd**, and **3-nbd**) are shown in Chart 1. Recently, Masuda's group demonstrated that rhodium catalysts that contain a strongly  $\pi$ -acidic diene, namely, tetrafluorobenzobarrelene (tfb), show higher catalytic activity and turnover frequency (TOF) than their nbd analogues (Chart 1). For instance,  $[(\text{tfb})\text{RhCl}_2]$  (**1-tfb**) achieves complete consumption of monosubstituted acetylenes in a shorter reaction time than  $[(\text{nbd})\text{RhCl}_2]$  (**1-nbd**), indicating higher TOF with **1-tfb**.<sup>8</sup> Complex **1-tfb** can be derivatized to other tfb–Rh catalysts, such as  $[(\text{tfb})\text{Rh}\{\text{C}(\text{Ph})=\text{CPh}_2\}(\text{PPh}_3)]$  (**2-tfb**) and  $[(\text{tfb})\text{Rh}(\eta^6\text{-Ph})\text{BPh}_3]$  (**3-tfb**). Catalyst **2-tfb** polymerizes PA in a living fashion to accomplish the most narrow molecular weight distribution (*i.e.*, polydispersity index 1.03) reported thus far.<sup>9</sup> Catalyst **3-tfb** shows higher activity than conventional **3-nbd**.<sup>10</sup> Optically pure dimethyl-introduced zwitterionic complexes **3-(S,S)-tfbMe<sub>2</sub>** and **3-(R,R)-tfbMe<sub>2</sub>** are effective for the helix-sense-selective polymerization of monosubstituted acetylene monomer **4** (Scheme 1).<sup>11</sup> Complex **3-tfb** is converted into a cationic derivative  $[(\text{tfb})\text{Rh}(\text{PPh}_3)_2][\text{BPh}_4]$  by the reaction of **3-tfb** with  $\text{PPh}_3$ , which also induces the living polymerization of PA in the presence of amines.<sup>12</sup>

A few reports have addressed rhodium catalysts that have a variety of bidentate ligands composed of two different types of coordination sites (Chart 2). Jia and coworkers have demonstrated the activity of a neutral Rh catalyst bearing a phosphinosulfonamido ligand,  $[(\text{nbd})\text{Rh}(\text{Ph}_2\text{PCH}_2\text{CH}_2\text{NTs})]$  (**5**, Ts =  $\text{SO}_2\text{C}_6\text{H}_4\text{-p-Me}$ ), in the polymerization of PA.<sup>13</sup> Jiménez *et al.* investigated a series of cationic Rh catalysts coordinated by hemilabile  $\text{Ph}_2\text{P}(\text{CH}_2)_n\text{Z}$ -type bidentate ligands (**6**,  $n = 2$  or 3; Z = OMe, NMe<sub>2</sub>, SMe) that polymerize PA and its derivatives

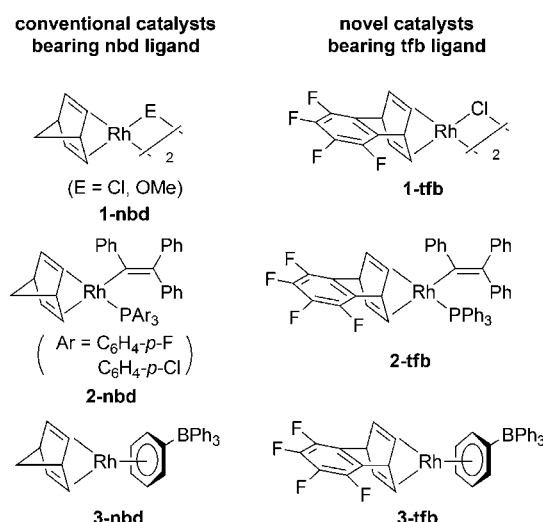
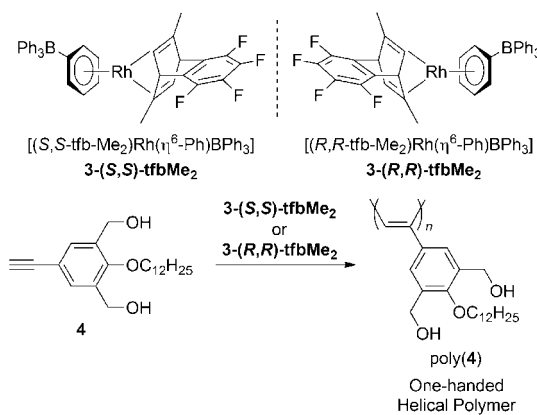


**Chart 1** Conventional nbd–Rh catalysts and newly investigated tfb–Rh catalysts.



**Scheme 1** Helix-sense-selective polymerization of PA derivative **4** by the chiral Rh zwitterionic catalyst, **3-(S,S)-tfbMe<sub>2</sub>** and **3-(R,R)-tfbMe<sub>2</sub>**.

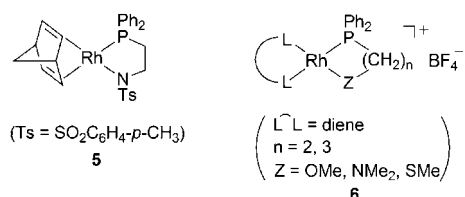
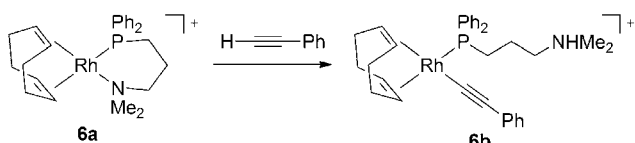


**Chart 2** The Rh catalysts bearing P-L type bidentate ligands.

efficiently.<sup>14</sup> Using NMR spectroscopy, they were able to directly observe the initiating species in the polymerization of PA using the catalyst containing the phosphinoamino ligand. The phenylethynyl Rh species **6b** is formed in the reaction of **6a** (diene = 1,5-cyclooctadiene (cod), *n* = 3, Z = NMe<sub>2</sub>) with PA, along with the formation of an ammonium moiety derived from the bidentate ligand and an acetylenic terminal proton of PA. Prior to this, it had been revealed that Rh acetylidyne-type complexes form in the reaction of certain complexes with acetylenic monomers.<sup>15,16</sup> This is the first case demonstrating that a reaction forming the Rh-acetylidyne is driven by the formation of ammonium salt (Scheme 2). Complex **6** with diene = tfb, *n* = 3, and Z = NMe<sub>2</sub> can achieve quasi-living polymerization of PA in the presence of 4-(*N,N*-dimethylamino)pyridine. This work also contributes to the following study regarding branched poly(PA) formed with the same catalyst as reported by Jiménez and Collins *et al.*<sup>17</sup>

Other polymerization catalysts based on Rh complexes are summarized in Chart 3. Rh complexes bearing 1,4,7-triazacyclononane (**7** and **8**) have been well-characterized and are utilized as polymerization catalysts for PA.<sup>18</sup> The Rh carbene complex **9** is synthesized by the reaction of [(cod)Rh(μ-OMe)]<sub>2</sub> with an ionic liquid, namely, 1-butyl-3-methylimidazolium halide, and is active in the catalytic polymerization of PA.<sup>19</sup> New



**Scheme 2** The formation of phenylethynyl species **6b** by the reaction of **6a** and excess PA.

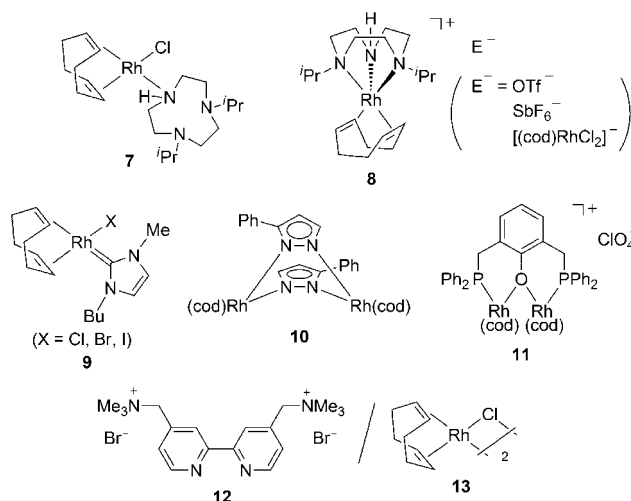


**Chart 3** Rh-based catalysts for the polymerization of monosubstituted acetylene monomers.

bimetallic complexes **10** and **11** show catalytic activity in the polymerization of PA.<sup>20,21</sup> Water-soluble cationic bipyridine **12** enables the recovery and reuse of a conventional catalyst, [(cod)RhCl]<sub>2</sub> (**13**), which polymerizes PA in aqueous conditions under air.<sup>22</sup> It has also been reported that the conventional complex **13** is incorporated in a spherical protein called ferritin. The apo-Fr-containing Rh-nbd complex obtained induces the polymerization of PA in the case of the protein to give the corresponding polymer with a narrower molecular weight distribution than that with catalyst **13** alone.<sup>23</sup>

Recently, a few heterogeneous Rh catalysts have been reported. Trzeciak's group demonstrated rhodium nanoparticles stabilized by polyvinylpyrrolidone exhibit catalytic activity in the polymerization of PA.<sup>24</sup> The stereochemistry of the polymer produced with this catalyst is purely *cis*-transoidal. The progress in polymerization can be monitored by atomic force microscopy (AFM) and transmission electron microscopy (TEM). This report includes the first detection of a spectacular helical PPA using AFM imaging. Son and Sweigart's group reported that the nanoparticles composed of the (benzoquinone)Rh(cod) complex and aluminium compounds catalyze the polymerization of PA. The catalyst nanoparticles can be recovered by centrifugation, and the recovered nanoparticles show almost the same activity.<sup>25</sup>

**1.1.2 Group 10 transition metal catalysts.** Darkwa's group investigated a series of new Pd catalysts, **14–18**, as listed in Chart 4. These Pd catalysts oligomerize or polymerize PA to derive poly(PA) in moderate to high yields. A series of catalysts (**14**) in conjunction with silver triflate show moderate activity in the oligomerization of PA.<sup>26</sup> Catalysts **15–18** also require activation with silver triflate in the polymerization of PA. The effect of the substituents (R) on the pyrazole/pyrazolyl ligands is significant, and it was observed that bulkier groups are more favorable for high monomer conversions.<sup>27</sup>

Ni-based catalysts (**19** and **20**, shown in Chart 5) are activated by excess MAO (methylaluminoxane) to oligomerize PA.<sup>28</sup> This yields a corresponding oligomer, with up to 60% yield. Catalyst **20** with R = C<sub>6</sub>H<sub>3</sub>-2,6-<sup>i</sup>Pr<sub>2</sub> results in the highest molecular weight

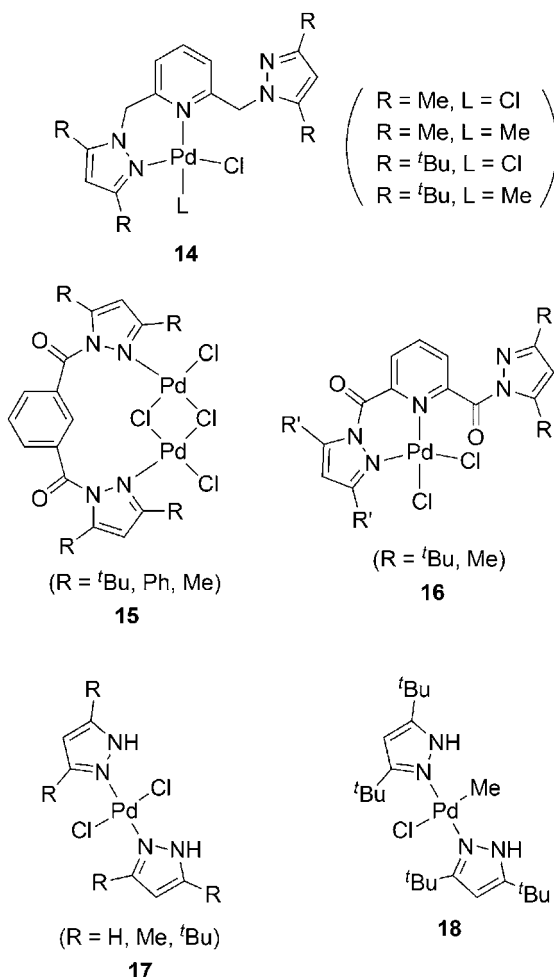


Chart 4 Novel Pd catalysts bearing pyrazole/pyrazolyl ligands.

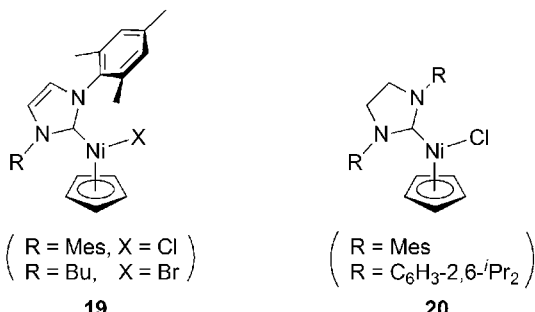


Chart 5 Novel Ni catalysts bearing imidazol-2-ylidene moieties.

polymer ( $M_n = 13\,600$ ) but also forms lower molecular weight oligomers, while the other catalysts yield monodisperse polymers with a smaller size range, with average molecular weights of less than 1600.

**1.1.3 Group 8 transition metal catalysts.** Regarding this category of catalysts, recent investigations have focused on ruthenium chemistry. A series of Ru carbene complexes listed in Chart 6 catalyze the polymerization of *o*-substituted PAs, as represented by (*o*-isopropoxy)phenylacetylene (Chart 7).<sup>29</sup> In particular, the Grubbs–Hovayda catalyst 22 results in the highest

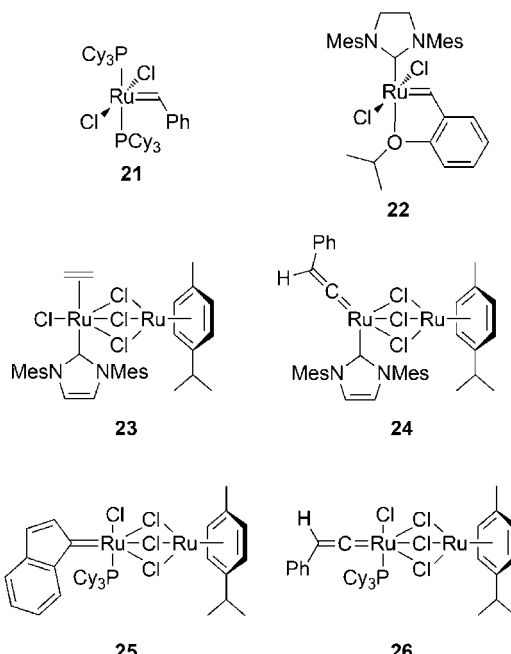


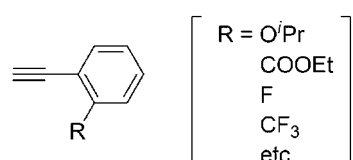
Chart 6 Ruthenium carbene catalysts for the polymerization of mono-substituted acetylenic monomers.

yield (72%) of the corresponding polymer among all reports on the treatment of simple acetylenic compounds with Ru-catalyzed polymerization. The substituents at the *ortho*-position of PA-type monomers are assumed to serve as supportive ligands that maintain and prolong the life of unstable propagating carbene species.

Another Ru carbene complex 27 (Chart 8) was reported to catalyze the oligomerization of PA and its derivatives into linear oligomers containing both positively charged and uncharged imidazolium end-groups.<sup>30</sup> The  $M_w$  values of the formed oligomers are less than 670.

**1.1.4 Group 6 transition metal catalysts.** (Arene)Mo(CO)<sub>3</sub> complexes can be activated by UV irradiation or by heating at high temperatures to polymerize monosubstituted acetylenes such as PA.<sup>2</sup> Santhosh and coworkers have found that these complexes can also be activated by the addition of an electron acceptor, namely, chloranil, in the case of (toluene)Mo(CO)<sub>3</sub>.<sup>31</sup> This catalytic system is applicable to ring-substituted PAs, such as *p*-BrPA, *p*-NO<sub>2</sub>PA, and *p*-MeOPA.

It was shown that a molybdenum amide complex having the  $\beta$ -agostic NSi–H $\cdots$ Mo complex 28 (Chart 9) polymerizes PA with moderate efficiency (TON = 34 and TOF = 2).<sup>32</sup>

Chart 7 *o*-Substituted PA derivatives polymerizable with Ru carbene catalysts 21–26.

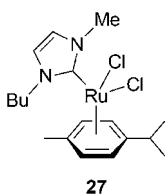


**Chart 8** Ru imidazolylidene catalyst.

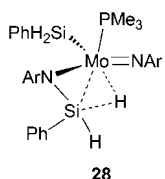


**Chart 9** Structure of a Mo amido complex having agostic NSi–H $\cdots$ Mo moiety.

Heterogeneous Mo catalysts supported by siliceous mesoporous molecular sieves can successfully polymerize alkynes.<sup>33</sup> Two types of Mo catalysts have been studied, which are based on the  $\text{MoO}_3$  and Schrock carbenes,  $\text{Mo}(\text{=CHCMe}_2\text{Ph})(\text{=N-C}_6\text{H}_3-2,6-\text{iPr}_2)[\text{OCMe}(\text{CF}_3)_2]_2$ . The latter exhibits high activity in the polymerization of 1-hexyne.

The quadruply bonded ditungsten complexes  $\text{Na}_4[\text{W}_2\text{Cl}_8(\text{THF})_x]$  and  $[\text{WCl}_4(\text{thf})_2]$  have been demonstrated to show catalytic activity in the polymerization of mono- and disubstituted acetylene monomers.<sup>34</sup> In particular,  $\text{Na}_4[\text{W}_2\text{Cl}_8(\text{THF})_x]$  shows high activity and achieves high yields of corresponding polymers with high molecular weights, with a  $M_n$  of 105 000 at most in the case of poly(*tert*-butylacetylene). Related triply bonded ditungsten complexes such as  $\text{A}_3[\text{W}_2(\mu\text{-Cl})_3\text{Cl}_6]$  ( $\text{A}^+ = \text{Bu}_4\text{N}^+$ ) and  $\text{Na}[\text{W}_2(\mu\text{-Cl})_3\text{Cl}_4(\text{THF})_2]$  also show catalytic activity on the polymerization of several mono-substituted acetylenes.<sup>35</sup>

## 2 Monosubstituted acetylenes: secondary structures and functions of monosubstituted acetylene polymers

Naturally occurring biomacromolecules, including proteins and DNA, commonly contain helical conformations, which are essential for carrying out their sophisticated and fundamental functions. Synthetic helical polymers have attracted much attention due to their ability to exhibit sophisticated features based on regulated structures that are similar to biomacromolecules. In particular, conjugated helical polymers such as polyisocyanides,<sup>36</sup> polysilanes,<sup>37-39</sup> and polyacetylenes<sup>40-43</sup> have been intensively studied because of their photo-electronic functions, which are useful in industrial applications.

Helical polymers of monosubstituted acetylenes were first synthesized with an Fe catalyst.<sup>44</sup> Since the development of Rh(i) complexes<sup>45-47</sup> and  $[\text{Rh}(\text{nbd})\text{Cl}]_2$ -triethylamine<sup>48</sup> as catalysts for PA polymerization, these Rh complexes have been most commonly used as catalysts for the stereospecific polymerization of monosubstituted acetylenes due to their high tolerance towards various polar functional groups. The substituted polyacetylenes that are formed have *cis*-stereoregular double bonds in the main chains. The head-to-tail contents of Rh-based

monosubstituted acetylene polymers are estimated to be around 90% according to pyrolysis gas chromatography.<sup>49</sup> This section overviews the recent studies on the secondary structures and functions of Rh-based monosubstituted acetylene polymers.

## 2.1. Poly(PA) derivatives

A wide variety of poly(PA) derivatives adopt helical conformations (Chart 10). Achiral poly(PAs) having carboxylic groups and crown ether moieties (**29a** and **29b**) predominantly induce one-handed helical structures by the addition of optically active compounds such as esters and the ammonium salts of amino acids.<sup>43</sup> Helix-sense-selective polymerization is achieved using optically active amines as cocatalysts to yield poly(PA)s substituted by bis(hydroxymethyl) groups with biased helix sense,<sup>50-52</sup> wherein intramolecular hydrogen bonding between the hydroxy groups stabilizes the helical structure. Anion recognition systems are constructed based on the interaction between **29c**<sup>53</sup> and **29d**.<sup>54</sup> Alanine-derived **29e** furnishes the twisting cables, spiral ribbons, spherical vesicles, and helical nanotubes.<sup>55</sup> *N*-Methylvaline-derived **29f** catalyzes the asymmetric reduction of aromatic ketimines.<sup>56</sup> The color and helical structures of **29g** film are tuned by exposure to organic solvent vapor and heat.<sup>57,58</sup>

Chart 11 summarizes some recent examples of poly(PA) derivatives that exhibit electronic and photo-functions.<sup>59-61</sup> The relationship between the spin-orbit coupling constant and *g*-values of poly(*para*-haloPA)s is examined.<sup>62</sup> Carbon nanotubes interact with **29h** and **29i**, which have carbazole/fluorene moieties by electron transfer,<sup>63</sup> and form hybrids with **29j** and **29k**, which have pyrene<sup>64</sup> and ferrocene<sup>65</sup> moieties. A film of **29h** undergoes electrochemical crosslinking.<sup>66</sup> Polyradicals **29l**<sup>67</sup> and **29m**<sup>68</sup> exhibit redox properties and excellent reversible charge/discharge

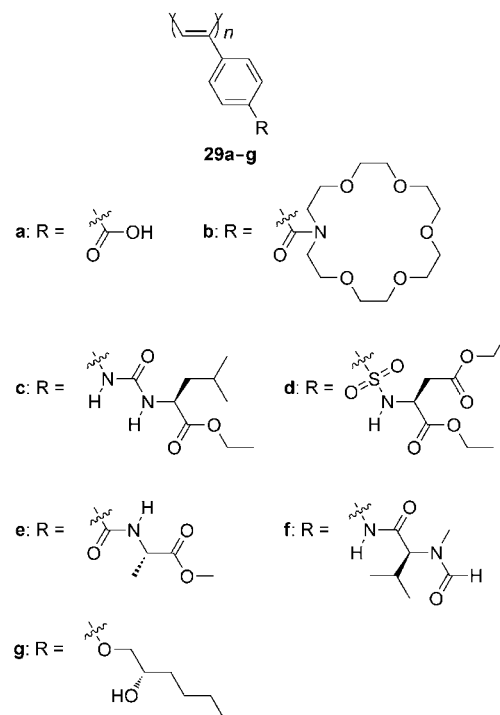


**Chart 10** Poly(PA) derivatives that adopt helical conformations.

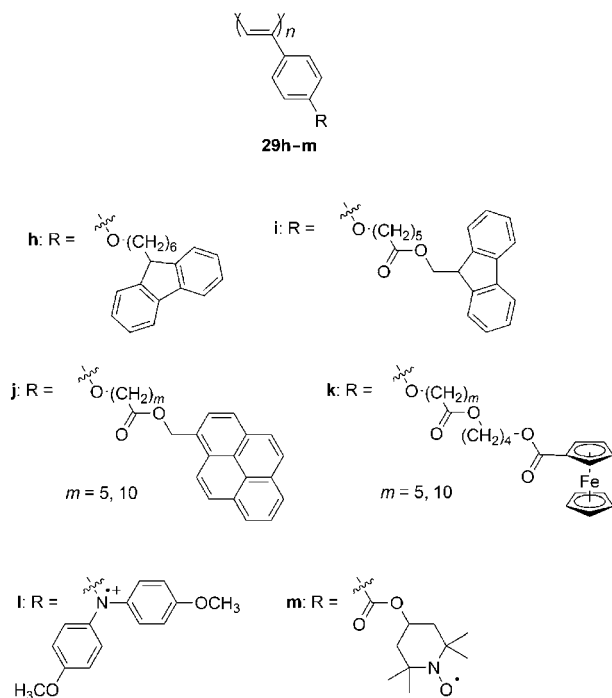


Chart 11 Electronic and photo-functional poly(PA) derivatives.

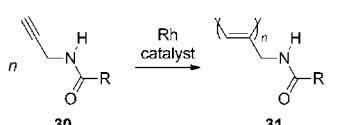
properties and thus are expected to become organic polymer batteries.

In addition to poly(PA) derivatives, polyacetylenes substituted with naphthalene,<sup>69</sup> pyrene,<sup>70</sup> and carbazole<sup>59,71–73</sup> moieties are synthesized, and their photoelectronic properties are examined. These polymers feature UV-vis absorption at long wavelength regions and exhibit large luminescence due to the long conjugation between the polyacetylene backbones and the polyaromatic side chains compared to poly(PA) derivatives.

## 2.2. Poly(*N*-propargylamide) derivatives

*N*-Propargylamides (**30**) efficiently undergo polymerization with Rh catalysts to give *cis*-stereoregular poly(*N*-propargylamide)s (**31**, Scheme 3). When the substituent R is optically active, **31** predominantly forms helices with a one-handed screw sense due to the steric repulsion between the side chains as well as intramolecular N–H···O=C hydrogen bonding (Fig. 1).<sup>74</sup> Since the first report of helix formation of **31** in 2001, *ca.* 50 papers related to poly(*N*-propargylamide)s have been published.

Recent examples of helical poly(*N*-propargylamide)s include **32a**, which is derived from optically active hydroxycarboxylic acids (Chart 12). Polymer **32a** tends to adopt a helical conformation in polar solvents such as DMF, while this does not happen in nonpolar solvents such as CHCl<sub>3</sub>.<sup>75</sup> The opposite trend is true for poly(*N*-propargylamide)s that do not contain hydroxy



Scheme 3 Polymerization of *N*-propargylamide.

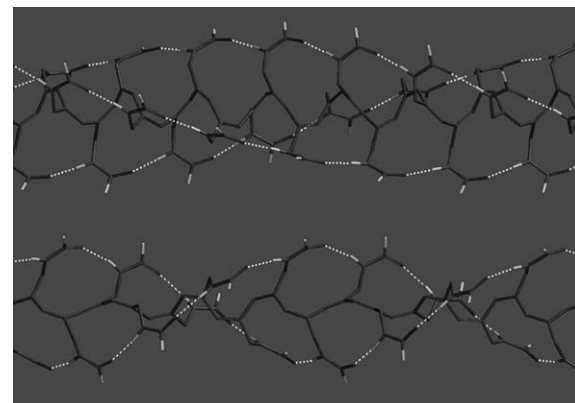


Fig. 1 Possible conformations of tightly (top) and loosely (bottom) twisted helical *cis*-stereoregular poly(*N*-propargylamide) [–CH=–C(CH<sub>2</sub>NHCOH)–]<sub>n</sub>, which accompany helically arranged intramolecular hydrogen-bonding strands (dotted lines) formed between the amide groups at the *i*<sup>th</sup> and (*i*+3)<sup>th</sup> units (top) and the *i*<sup>th</sup> and (*i*+2)<sup>th</sup> units (bottom). Methine and methylene hydrogen atoms are omitted for clarity.

groups. It is likely that the hydroxy groups of **32a** prevent polar solvents from disturbing the intramolecular hydrogen bonding between the amide groups. Gels that consist of mainly helically twisted **32a** (*m* = 0) derived from lactic acid recognize chirality more prominently than analogous polymer gels that do not contain helices. The hydroxy groups of **32a** can be protected by esterification. The bulkiness of the R' substituent of **32b** affects the helical conformation. Comparing **32b** with R' = –CH<sub>2</sub>Ph, –CHPh<sub>2</sub>, and –CPh<sub>3</sub>, it can be seen that the polymer bearing more phenyl groups forms a looser helix.<sup>76</sup> Bulky side chains make the polymer chain flatter. Polymer **32c**, which carries azobenzene moieties in the side chains, is synthesized from lactic acid.<sup>77</sup> The CD spectra simulated by the molecular orbital method agree with the experimental spectra and indicate the arrangement of azobenzene moieties in a mutual chiral geometry of a one-handed screw sense. The *trans*-azobenzene moieties in

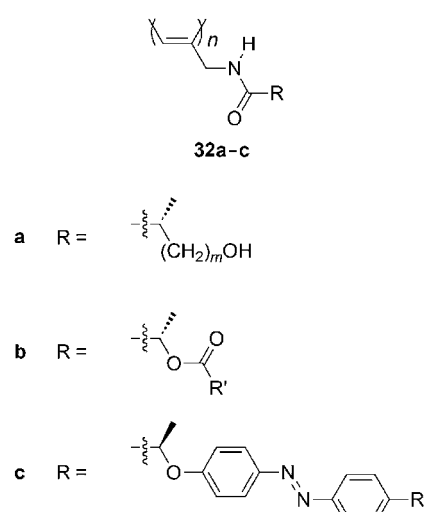


Chart 12 Poly(*N*-propargylamide)s derived from optically active hydroxycarboxylic acids.

the side chain isomerize into *cis*-forms upon UV irradiation, while the helical structure of the main chain is not affected as much. The *cis*-azobenzene moieties reisomerize into *trans*-forms upon visible-light irradiation. Simultaneously, the azobenzene moieties recover the initial chiral arrangement at the side chains. The polymer forms a cholesteric liquid crystal.

Amino acids are a versatile source of chirality for organic synthesis. Synthetic polymers containing amino acid moieties show useful functions such as chiral separation, bioactivity, and stimuli-responsiveness in a manner similar to peptides and proteins.<sup>78</sup> A series of helical polyacetylenes substituted with amino acid moieties are synthesized, some of which invert the helical sense by external stimuli such as temperature,<sup>79</sup> solvent,<sup>80,81</sup> and pH.<sup>82</sup> Fluorescence emission can be controlled according to the secondary structure of the polymers.<sup>83,84</sup> Ornithine- and lysine-based helical poly(*N*-propargylamide)s **32d** and **32e** can change the helix degree in response to an acid (Chart 13).<sup>85</sup> Gels based on these polymers recognize chirality.<sup>86</sup>

Synthetic polymers that have sugar residues have attracted much attention due to their potential applications in biologically active materials. Fluorescent-dye-labelled amphiphilic helical copolymers (**33**) are synthesized by the copolymerization of *N*-propargylamides that contain the galactose residue,<sup>87</sup> lauryloyl group, and rhodamine B dye moieties (Chart 14).<sup>88</sup> Human aortic endothelial cells (HAECS) are cultured in a medium containing **33**. Cell uptake of the copolymer is confirmed by red fluorescence emission from each of the HAECS. An amylose-grafted polyacetylene is also synthesized chemoenzymatically, utilizing the polymerization of *N*-propargylamide.<sup>89</sup>

The microemulsion polymerization of *N*-propargylamides provides nanoscale particles consisting of helical polymers in aqueous medium.<sup>90</sup> These particles show a higher preference for a one-handed screw sense compared with the polymers that are synthesized in organic solvents. The subsequent radical polymerization of vinyl monomers yields nanoparticles consisting of a core that is composed of a substituted helical polyacetylene and a shell that is composed of a vinyl polymer.<sup>91</sup> Achiral *N*-propargylamides undergo aqueous emulsion polymerizations in chiral micelles consisting of sodium dodecyl sulfate and an amino acid to yield optically active helical polymer emulsions.<sup>92</sup>

Optically active *N*-propargylphosphonamidates (**34**) having a *P*-chiral center are synthesized and polymerized to obtain the polymers shown in Chart 15.<sup>93–95</sup> The formed polymers adopt a helical conformation that is stabilized by intramolecular N–H···O=P hydrogen bonding. The predominance of the screw sense is determined by the *P*-chirality rather than the *C*-chirality.

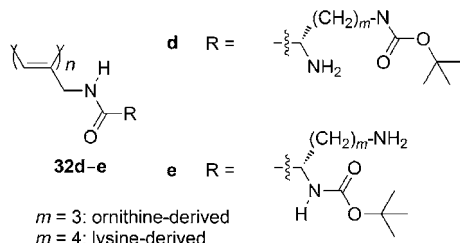


Chart 13 Ornithine- and lysine-based poly(*N*-propargylamide)s.

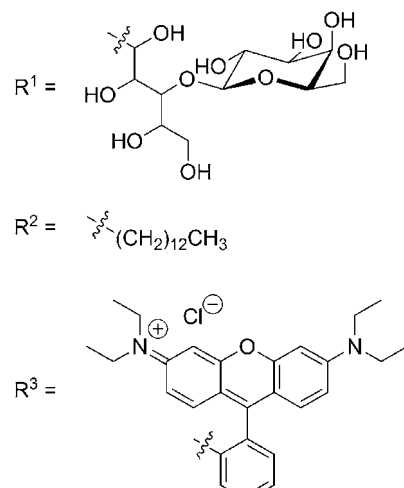
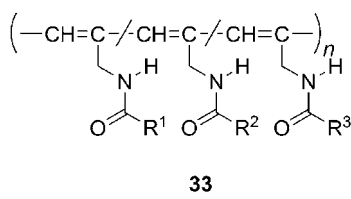


Chart 14 Amphiphilic copolymers of *N*-propargylamides labelled with a fluorescent dye.

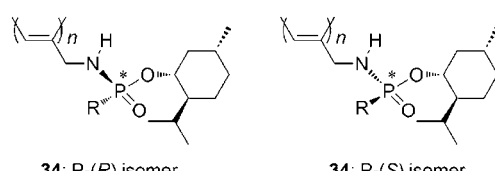
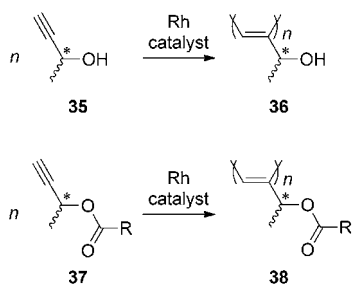


Chart 15 *P*-Chiral poly(*N*-propargylphosphonamidate)s.

### 2.3. Poly(1-methylpropargyl ester) derivatives

Propargyl alcohol is the most simple acetylene monomer that has a hydroxy group; it undergoes polymerization with Pd and Ni catalysts.<sup>96–100</sup> 1-Methylpropargyl alcohol (**35**) is a chiral derivative of propargyl alcohol and has various applications in the field of organic chemistry; *e.g.*, it has been utilized for the regioselective carbometalation with Grignard reagents affording 2-substituted allylic alcohols,<sup>101</sup> in the synthesis of 2-substituted indoles *via* Sonogashira coupling cyclization,<sup>102</sup> as a precursor of chiral allenylzinc and indium reagents,<sup>103</sup> and in the synthesis of phosphinoyl 1,3-diene.<sup>104</sup> The polymerization of **35** and the ester derivatives (*i.e.*, **37**) was first reported in 2007 (Scheme 4).<sup>105</sup> The obtained polymers **36** and **38** form helices, and the helical conformation of **38** having ester groups is thermally more stable than that of **36**, which contains hydroxy groups.<sup>106</sup> The remarkable ability of such a small chiral moiety to induce helicity is most likely due to the location of the chiral group adjacent to the main chain. In other words, the presence of a chiral group in close proximity to the main chain has enough of an effect to induce a helix that is stabilized by steric repulsion between the side chains.



**Scheme 4** Polymerization of 1-methylpropargyl alcohols and esters.

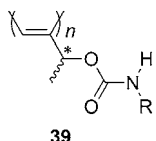


**Chart 16** Poly(1-methylpropargyl-*N*-alkylcarbamate)s.

Helical poly(1-methylpropargyl ester)s having various functional groups are synthesized. They include liquid crystalline polymers having cholesteryl groups,<sup>107,108</sup> fluorescent polymers having carbazole<sup>109</sup> and pyrenyl<sup>110</sup> groups, photo-isomerizable polymers having azobenzene moieties,<sup>111</sup> and stimuli-responsive polymers having amino acid moieties.<sup>112</sup> Graft copolymers consisting of a helical polyacetylene backbone and poly(methyl methacrylate)/poly(styrene) side chains are synthesized by the polymerization of 1-methylpropargyl ester-based macromonomers.<sup>113,114</sup>

Poly(1-methylpropargyl-*N*-alkylcarbamate)s (39, Chart 16) utilize intramolecular N—H···O=C hydrogen bonding in addition to the steric repulsion between the methyl groups adjacent to the main chain.<sup>115</sup> The polymers form a pseudo hexagonal columnar structure by self-assembly or self-organization in the solid state. Thus, chiral 1-methylpropargyl alcohol is a simple but extremely powerful and useful helical source for substituted polyacetylenes.

### 3 Disubstituted acetylenes

#### 3.1 Polymerization

The polymerization behavior of disubstituted acetylene monomers has been sufficiently clarified, and the related studies and reviews are cited for ref. 2–4 and 6. The general relationship between the type of catalyst and the structure of the disubstituted acetylene monomers is as follows. In general, disubstituted acetylenes are sterically more crowded than their mono-substituted counterparts, and consequently, their effective polymerization catalysts are restricted virtually to group 5 and 6 transition metal catalysts; Rh catalysts are generally not effective. Among disubstituted acetylenes, those with less steric hindrance, specifically internal alkynes, polymerize with Mo and W catalysts, while they tend to yield cyclotrimers with Nb and Ta catalysts. 1-Chloro-alkynes and 1-chloro-2-phenylacetylene polymerize with only Mo catalysts. In contrast, sterically crowded disubstituted acetylenes such as 1-trimethylsilyl-1-propyne do not polymerize with Mo or W catalysts, but they do polymerize with Nb and Ta catalysts. Diphenylacetylene and its ring-substituted derivatives are even more sterically hindered and

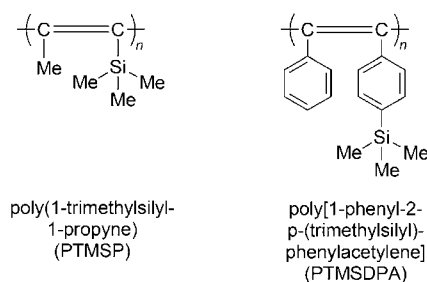
polymerize only with the TaCl<sub>5</sub>-cocatalyst system. 1-Phenyl-1-alkynes have intermediate steric hindrance and hence polymerize with Nb, Ta, and W catalysts.

The polymers from disubstituted acetylenes that have two identical groups or two groups of similar sizes are generally insoluble in any solvent. Most polymers from disubstituted acetylenes are colorless, although some aromatic polymers are yellow in color. While the controlled polymerization of mono-substituted acetylenes is applied to precision polymer syntheses such as living polymers, star polymers, and polymer brushes, this is not the case with disubstituted monomers because living polymerization is still not possible with disubstituted acetylene monomers. Cylindrical polymer brushes composed of a poly(diphenylacetylene) main chain and poly(oxyethylene) side chains have been prepared using the macromonomer and so-called ‘graft-from’ methods.<sup>116</sup>

#### 3.2 Gas-permeable polymers

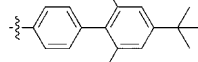
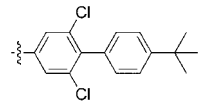
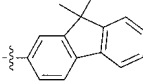
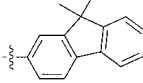
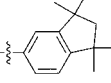
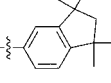
Polymers from disubstituted acetylenes have been intensively examined for their practical application as gas-permeable materials.<sup>117–120</sup> These studies are motivated by the extremely high gas permeability of poly(1-trimethylsilyl-1-propyne) (PTMSP, Chart 17),<sup>120</sup> which is the most permeable material available among all polymers. The oxygen permeability coefficient ( $P_{O_2}$ ) of PTMSP ranges from 4000 to 9000 barrers, which is about ten times larger than that of poly(dimethylsiloxane). In addition to its high permeability, the ability of PTMSP to yield a free-standing film and its gas permeation mechanism, which is different from that of poly(dimethylsiloxane), have attracted much attention among membrane scientists. Poly[1-phenyl-2-*p*-(trimethylsilyl)phenylacetylene] (PTMSDPA, Chart 17) is a typical, highly gas-permeable poly(diphenylacetylene) and features high thermal stability compared to PTMSP.

Examples of highly gas-permeable substituted polyacetylenes are shown in Table 1. The  $P_{O_2}$  values and oxygen/nitrogen selectivities ( $P_{O_2}/P_{N_2}$ ) (25 °C) of about 100 substituted polyacetylenes have been measured so far.<sup>117,118,120</sup> Among these substituted polyacetylenes, many of the polymers with large  $P_{O_2}$  values contain spherical substituents, such as *t*-Bu, Me<sub>3</sub>Si and Me<sub>3</sub>Ge groups. In contrast, a majority of the less permeable polyacetylenes possess long *n*-alkyl groups. When the phenyl group is a main substituent, the gas permeability of the resulting polyacetylenes is usually considerably lower. Among commercially available oxygen-permeable polymer membranes, poly(dimethylsiloxane) is known to be most permeable to oxygen, with a  $P_{O_2}$  value of 600 barrers (25 °C). As seen in Table 1, substituted polyacetylenes are very permeable to oxygen. The



**Chart 17** Structures of PTMSP and PTMSDPA.

**Table 1** Oxygen permeability coefficients ( $P_{O_2}$ ) and  $P_{O_2}/P_{N_2}$  of gas permeable substituted polyacetylenes

No	$R^1$	$R^2$	$P_{O_2}/\text{barrier}^a$	$P_{O_2}/P_{N_2}$	Reference
1	Me	SiMe <sub>3</sub>	$4 \times 10^3$ to $9 \times 10^3$	1.8	120
2	Me	SiEt <sub>3</sub>	860	2.0	121
3	Me	SiMe <sub>2</sub> Et	500	2.2	121
4	Me	SiMe <sub>2</sub> -i-C <sub>3</sub> H <sub>7</sub>	460	2.7	121
5	Me	GeMe <sub>3</sub>	7800		122
6	Ph	C <sub>6</sub> H <sub>4</sub> - <i>p</i> -SiMe <sub>3</sub>	1100–1550	2.1	117 and 118
7	Ph	Ph	910	2.2	123
8	Ph	C <sub>6</sub> H <sub>4</sub> - <i>m</i> -SiMe <sub>3</sub>	1200	2.0	124
9	Ph	C <sub>6</sub> H <sub>4</sub> - <i>m</i> -GeMe <sub>3</sub>	1100	2.0	117 and 118
10	Ph	C <sub>6</sub> H <sub>4</sub> - <i>p</i> - <i>t</i> -C <sub>4</sub> H <sub>9</sub>	1100	2.2	117 and 118
11	$\beta$ -Naphthyl	C <sub>6</sub> H <sub>4</sub> - <i>p</i> -SiMe <sub>3</sub>	3500	1.8	117 and 118
12	$\beta$ -Naphthyl	Ph	4300	1.6	117 and 118
13	C <sub>6</sub> H <sub>4</sub> - <i>p</i> -F	C <sub>6</sub> H <sub>4</sub> - <i>p</i> -SiMe <sub>3</sub>	2900	1.5	124
14	C <sub>6</sub> H <sub>4</sub> - <i>p</i> -F	Ph	3000	1.4	124
15	C <sub>6</sub> H <sub>3</sub> - <i>m,p</i> -F <sub>2</sub>	C <sub>6</sub> H <sub>4</sub> - <i>p</i> -SiMe <sub>3</sub>	3600	1.5	124
16	C <sub>6</sub> H <sub>3</sub> - <i>m,p</i> -F <sub>2</sub>	Ph	3800	1.3	124
17	Ph	C <sub>6</sub> H <sub>4</sub> - <i>p</i> -OSiMe <sub>2</sub> - <i>t</i> -Bu	160	3.2	125
18	Ph	C <sub>6</sub> H <sub>4</sub> - <i>p</i> -OH	8.0	3.3	125
19	Ph		1100	2.1	126
20	Ph		1400	1.9	126
21	Ph		4800	1.5	127
22	C <sub>6</sub> H <sub>3</sub> - <i>m,p</i> -F <sub>2</sub>		6600	1.3	127
23	Ph		14 400	1.2	128
24	C <sub>6</sub> H <sub>3</sub> - <i>m,p</i> -F <sub>2</sub>		18 700	1.1	128

<sup>a</sup> 1 barrer =  $1 \times 10^{-10}$  cm<sup>3</sup>(STP) cm/(cm<sup>2</sup> s cmHg).

high gas permeability of polyacetylenes is attributable to their high free volume, which is presumably derived from their low cohesive energy structure, stiff main chain and spherical substituents.

Poly(diphenylacetylene)s are thermally very stable ( $T_0 > 400$  °C) and possess a film-forming ability. The ease in modifying ring substituents provides an opportunity to tune the permeability as well as the solubility and second-order conformation of the polymer. The permeability of poly(diphenylacetylene)s depends significantly on the shape of the ring substituents.<sup>117,118</sup> Specifically, those with bulky ring substituents such as *t*-Bu, Me<sub>3</sub>Si and Me<sub>3</sub>Ge groups (nos. 6 and 8–10 in Table 1) exhibit very large  $P_{O_2}$  values of up to 1000–1500 barrers, which is about one fourth of that of PTMSP and approximately twice as large as that of poly(dimethylsiloxane).

While poly(diphenylacetylene) is insoluble in any solvent, its derivatives with bulky ring-substituents are usually soluble in common solvents such as toluene and chloroform and derived membranes by solution casting. A poly(diphenylacetylene) membrane has been prepared by the desilylation of a PTMSDPA membrane that was catalyzed by trifluoroacetic acid.<sup>123</sup> The prepared polymer membrane shows high thermal stability, insolubility in any solvent, and high gas permeability (e.g., an oxygen permeability of 910 barrers at 25 °C; no. 7 in Table 1). The high gas permeability of poly(diphenylacetylene) seems to be due to the generation of molecular-scale voids. In a similar way, poly(diphenylacetylene)s that contain various silyl groups such as Me<sub>2</sub>-i-PrSi, Et<sub>3</sub>Si and Me<sub>2</sub>-*n*-C<sub>8</sub>H<sub>17</sub>Si are soluble in common solvents, and poly(diphenylacetylene) membranes can be

obtained by desilylation from those membranes. These oxygen permeability coefficients (120–3300 barrers) are quite different from one another, despite having the same polymer structure. When the bulkier silyl groups are removed, the oxygen permeability tends to increase to a larger extent.

Poly[1-aryl-2-*p*-(trimethylsilyl)phenylacetylene]s [aryl = naphthyl, fluorenyl, phenanthryl] are soluble in common solvents and afford freestanding membranes.<sup>117,118</sup> These Si-containing polymer membranes are desilylated to yield the membranes of poly[1-aryl-2-phenylacetylene]s. Both the starting and the desilylated polymers show very high thermal stability and high gas permeability. For instance, the  $T_0$  and  $P_{O_2}$  values of poly(1-*p*-naphthyl-2-phenylacetylene) are 470 °C and 4300 barrers, respectively (no. 12 in Table 1).<sup>117,118</sup> Poly(diphenylacetylene)s with silyl groups and fluorine atoms are highly gas-permeable.<sup>124</sup> The fractional free volume (FFV) of poly[1-(4-fluoro)phenyl-2-*p*-(trimethylsilyl)phenylacetylene] is 0.28 and appreciably large (e.g., 0.26 of PTMSDPA). The oxygen permeability coefficient of poly[1-(4-fluoro)phenyl-2-*p*-(trimethylsilyl)phenylacetylene] is as high as 2900 barrers, which is about twice that of PTMSDPA (no. 13 in Table 1). The incorporation of fluorine atoms into PTMSDPA generally enhances gas permeability.

Disubstituted acetylenes with hydroxy groups do not polymerize because Ta and Nb catalysts are deactivated by polar groups such as hydroxy groups. In contrast, a protected monomer, that is, 1-phenyl-2-*p*-(*tert*-butyldimethylsiloxy)phenylacetylene, polymerizes to give a high molecular weight polymer.<sup>125</sup> This polymer is soluble in common organic solvents and provides a freestanding membrane. Desilylation of a poly[1-phenyl-2-*p*-(*tert*-butyldimethylsiloxy)phenylacetylene] membrane yields a poly(diphenylacetylene) that has free hydroxy groups. This is the first example of a highly polar group-carrying poly(diphenylacetylene). Unlike the starting polymer, poly(1-phenyl-2-*p*-hydroxyphenylacetylene) is insoluble in nonpolar solvents such as toluene and chloroform. The  $P_{CO_2}/PCH_4$  and  $P_{CO_2}/PN_2$  permselectivity ratios of the poly(1-phenyl-2-*p*-hydroxyphenylacetylene) membrane can be as large as *ca.* 46, while the  $P_{CO_2}$  is kept relatively high at 110 barrers.

Diarylacetylene monomers containing substituted biphenyl and anthryl groups have been synthesized and then polymerized with  $TaCl_5-nBu_4Sn$  catalyst to produce the corresponding poly(diarylacetylene)s.<sup>126</sup> The formed polymers are soluble in common organic solvents such as cyclohexane, toluene, and chloroform and have high thermal stability over 400 °C according to thermogravimetric analysis. These polymer membranes, especially those with twisted biphenyl groups, exhibit high gas permeability, *e.g.*, their  $P_{O_2}$  values range from 130 to 1400 barrers. The membranes that have two methyl or chlorine atoms in the biphenyl group show fairly high gas permeability ( $P_{O_2}$  1100 and 1400 barrers, respectively), mostly likely because the twisted biphenyl structure is useful in generating molecular scale voids (no. 19 and 20 in Table 1).

Diarylacetylenes having fluorenyl groups and other substituents (*i.e.*, trimethylsilyl, *tert*-butyl, bromine, and fluorine) also polymerize with  $TaCl_5-nBu_4Sn$ , forming high molecular weight polymers ( $M_w$  10<sup>5</sup> to 10<sup>6</sup>) in approximately 10–60% yields.<sup>127</sup> These polymers are soluble in common organic solvents and yield tough freestanding membranes by solution casting. These polymer membranes show high gas permeability, *e.g.*, the  $P_{O_2}$

value of the polymer that contains 9,9-dimethylfluorenyl and phenyl groups is as large as 4800 barrers (no. 21 in Table 1). The polymer membrane that possesses two fluorine atoms at the *meta* and *para* positions of the phenyl ring displays the highest oxygen permeability ( $P_{O_2}$  6600 barrers) among these types of polymers.

Acetylenic monomers containing indan and other groups also polymerize with the  $TaCl_5-nBu_4Sn$  catalyst.<sup>128</sup> Most of the formed polymers are soluble in common organic solvents and afford freestanding membranes by solution casting. Despite the absence of bulky spherical groups, polymethylated indan-containing polymer membranes show extremely high gas permeability. For instance, the  $P_{O_2}$  value of the polymer bearing 1,1,3,3-tetramethylindan and phenyl groups can reach 14 400 barrers (no. 23 in Table 1). In particular, the  $P_{O_2}$  values of the polymers having 1,1,3,3-tetramethylindan and either *p*-fluorophenyl or *p,m*-difluorophenyl groups reach 17 900 and 18 700 barrers, respectively, which are clearly larger than that of PTMSP.

PTMSP, which has long been known as the most gas-permeable polymer, is still being investigated with respect to various aspects of its permeation of gases and liquids. Research subjects in this area include membranes based on PTMSP for liquid–liquid separation;<sup>129</sup> the effect of direct-current discharge treatment on the surface properties of a PTMSP membrane;<sup>130</sup> crosslinking and stabilization of nanoparticle-filled PTMSP nanocomposite membranes for gas separations;<sup>131</sup> crosslinking PTMSP and its effect on physical stability;<sup>132</sup> gas transport properties of MgO-filled PTMSP nanocomposites;<sup>133</sup> bromination of PTMSP with different microstructures and properties of bromine-containing polymers;<sup>134</sup> pure and mixed gas  $CH_4$  and *n*- $C_4H_{10}$  permeability and diffusivity in PTMSP;<sup>135</sup> gas transport properties of PTMSP and ethylcellulose filled with different molecular weight trimethylsilsaccharides and the impact on fractional free volume and chain mobility;<sup>136</sup> Fourier transform infrared spectroscopy of PTMSP aging;<sup>137</sup> and free volume and interstitial mesopores in silica filled PTMSP nanocomposites.<sup>138</sup>

PTMSDPA, a disubstituted glassy acetylene-based polymer, exhibits higher permeabilities to organic vapors than to permanent gases due to its rigid polyacetylene backbone and bulky side groups, which provide a relatively high FFV value of 0.26.<sup>139</sup> The gas permeability and desilylation effect of poly(diphenylacetylene)s that have trimethylsilyl and alkyl groups have been studied.<sup>140</sup> Sulfonic acid groups have been introduced into poly(diphenylacetylene)s to yield ionic and hydrophilic polyacetylenes.<sup>141,142</sup> The degree of sulfonation usually ranges from 0.5 to 1.5 per repeating unit, and freestanding membranes can be obtained from the sulfonated polymers. Application of the membranes as proton-conducting fuel cell membranes has been examined.<sup>141</sup> These membranes can also be used as  $CO_2$  separation membrane materials.<sup>142</sup> The sulfonated polymers exhibit high  $CO_2$  permselectivity; *e.g.*, their  $CO_2/N_2$  separation factors are over 31. The sulfonated poly(diphenylacetylene) with the highest degree of sulfonation displays the highest  $CO_2/N_2$  ratio of 75.

### 3.3 Photoelectronic functions

In regard to photoelectronic functions, monosubstituted acetylene polymers have been studied more than disubstituted

acetylene polymers because they are generally more conjugated and coloured due to their less sterically demanding structure. However, considering the higher stability of the disubstituted acetylene polymers, they may be more suited for practical applications.

**3.3.1 Photoluminescence and electroluminescence.** Many studies on the photoluminescence of disubstituted acetylene polymers have been reported. Several recent studies are introduced here.

New poly(diphenylacetylene)s with alkoxy, silyl and fluorine groups (e.g., **40** in Chart 18) have been synthesized using W and Ta catalysts.<sup>143</sup> The polymer solutions emit a strong bluish-green light when photoexcited. The polymers containing electron-donating alkoxy groups show slightly longer fluorescence maxima compared to the polymers with the electron-withdrawing fluorine atoms. The effect of the alkyl chain length on the fluorescence of the poly(diphenylacetylene)s containing alkylsilane moieties (**41** in Chart 18) in their side chains has been studied.<sup>144</sup> Longer alkyl groups in the side chains of the polymer lead to longer fluorescence lifetimes. A longer alkyl group is also shown to be more effective than a shorter one in aligning the polymer chain parallel to the shearing direction.

A poly(diphenylacetylene) containing 1,2,3,4,5-pentaphenylsilole ( $\text{SiC}_4\text{Ph}_5$ ) pendants (**42** in Chart 18) has been synthesized, and its photoluminescence has been studied.<sup>145</sup> The ethynyl

group of the diphenylacetylene moiety polymerizes exclusively, resulting in a soluble polymer. The chloroform solution of the polymer shows a backbone emission centering at 522 nm, whereas the silole pendant is nonradiative at room temperature. Intramolecular rotations of the Ph groups on the silole chromophore. The intramolecular rotations, however, can be largely restricted through a cooling process of the polymer solution, which shows cooling-enhanced emission. Thus, the silole emission becomes dominant at lower temperatures.

$\alpha$ -Naphthalene-containing poly(diphenylacetylene)s with methylene spacers of different lengths ( $m = 4, 6$ , and  $8$ ) (e.g., **43** in Chart 18) have been synthesized. Although the  $\text{TaCl}_5-n\text{Bu}_4\text{Sn}$  catalyst results in insoluble products in low yields, the  $\text{WCl}_6-\text{Ph}_4\text{Sn}$  catalyst furnishes soluble polymers with high molecular weights ( $M_w$  up to  $5.0 \times 10^4$ ) in satisfactory yields of up to 62%.<sup>146</sup> When the polymers are photoexcited in THF solution, they emit strong green lights with high efficiencies up to 98%. No significant shifts in the photoluminescence spectra are observed, even though the polymers are cast into thin solid films, suggesting little involvement of aggregative or excimeric emission. A multilayer EL device has been constructed that emits a green light of 520 nm with a maximum external quantum efficiency of 0.16%. The spectral stability is outstanding; no recognizable change is observed in the EL spectrum, even when the device current is raised.

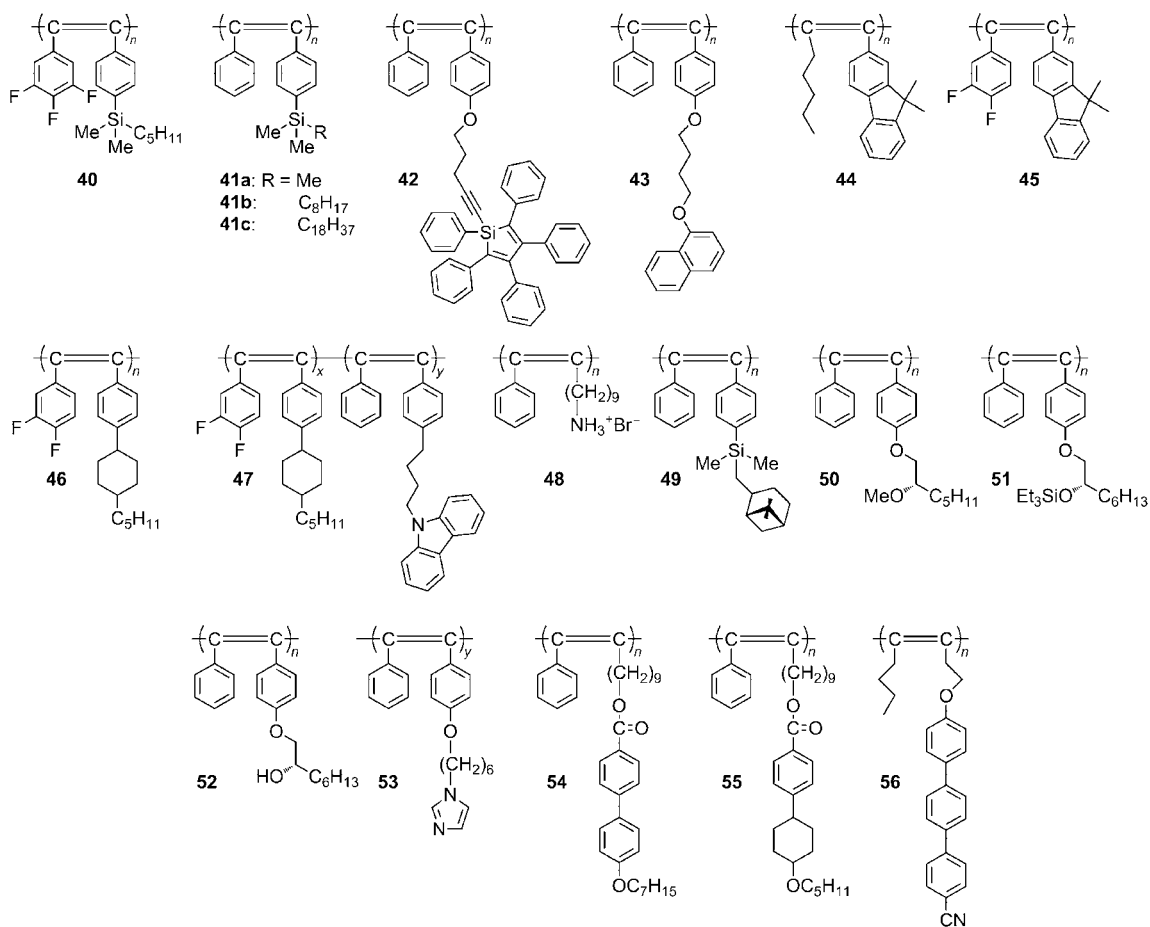


Chart 18 Structures of disubstituted acetylene polymers that show photoelectronic functions.

Novel fluorene-containing polymers, poly[(1-pentyl-2-(9,9-dimethylfluoren-2-yl)acetylene)] (**44** in Chart 18), and poly[1-(3,4-difluorophenyl)-2-(9,9-dimethylfluoren-2-yl)acetylene] (**45** in Chart 18), have been synthesized using  $TaCl_5$ -*n*-Bu<sub>4</sub>Sn as the catalyst.<sup>147</sup> These polymers show emission peaks from 402 to 590 nm. In addition, their electroluminescent properties have been studied in heterostructure light-emitting diodes (LEDs), using these polymers as an emitting layer. A device based on **45** exhibits an orange-red emission at 602 nm with a maximum luminescence of 923 cd m<sup>-2</sup> at 8 V. A device with the ITO/PEDOT/a mixture of **44** and **45** (98 : 2 wt ratio)/Ca/Al shows near-white emission. Its maximum luminance and current efficiency are 450 cd m<sup>-2</sup> at 15 V and 1.3 cd A<sup>-1</sup>, respectively.

For organic light-emitting diode (OLED) applications, novel poly(diphenylacetylene)s (*e.g.*, **46** in Chart 18), which exhibit air stability, better solubility in common organic solvents and higher luminescence than polyacetylene, have been examined as an emitter.<sup>148</sup> The devices have a maximum brightness of 827 candelas cd m<sup>-2</sup> at 12 V and a maximum current efficiency of 0.78 cd A<sup>-1</sup> at 9 V with a maximum luminescence at 536 nm.

Fluorine-containing poly(diphenylacetylene) (**46** in Chart 18) shows a large red shift in UV-vis absorption and PL emission and a very high luminescent efficiency compared to its counterpart, which lacks the two fluorine atoms.<sup>149</sup> The device performance can be improved using a light-emitting copolymer composed of **46** and a carbazole-bearing unit (**47** in Chart 18). A light-emitting diode of ITO/PEDOT/**47**/Ca/Al displays a maximum luminescence of 4230 cd m<sup>-2</sup> at 14 V and a maximum current efficiency of 3.37 cd A<sup>-1</sup> at 7 V.

Nanohybridization of inorganic semiconductors with organic conjugated polymers is expected to lead to the creation of new hybrids with combined advantages of the two components, namely, the high charge mobility of the inorganics and the ready processability of the organics. Poly(diphenylacetylene)s containing ammonium bromide moieties (**48**) and PbBr<sub>2</sub> provide a functional perovskite nanohybrid that shows a higher photoconductivity than its parent polymer **48** alone.<sup>150</sup>

**3.3.2 Chiral recognition and sensing.** Helices represent a typical secondary structure of polymers, and in cases in which one sense is predominant over the other sense, chirality is generated. Helical polymers can be categorised as stable or thermodynamic. Stable helical polymers have the potential to be used as stationary phases for high-performance liquid chromatography (HPLC) enantioseparation and as chiral membranes for selective permeation. The racemates with different configurations may pass through the molecular voids in the chiral membranes at different permeation rates, resulting in the separation of racemic mixtures. This possibility has been studied using a chiral membrane of polymer **49** with a one-handed helical conformation.<sup>151</sup> 2-Butanol is a small, not-so-polar molecule, and the direct separation of its racemates by using a chiral HPLC column is difficult. In the enantioselective permeation of racemic 2-butanol through the chiral membrane of **49**, it was proven that the (*R*)-isomer preferentially permeates through the chiral membrane in high selectivity ( $\alpha^R = 9.24$ ) and enantiomeric excess (ee = 80.5%).

Optically active poly(diphenylacetylene) derivatives, poly(4-((*S*)-2-methoxyoctyloxy)diphenylacetylene) (**50** in Chart 18), poly(4-((*S*)-2-triethylsiloxyoctyloxy)diphenylacetylene) (**51**), and

poly(4-((*S*)-2-hydroxyoctyloxy)diphenylacetylene) (**52**) have been synthesized, and their chiroptical and liquid crystalline properties have been examined.<sup>152</sup> The mirror image of the circular dichroic (CD) spectra of **50** and **51** in dilute solution indicates that their polymer backbones adopt a helical conformation with the opposite handedness. Polymer **52** prepared from **51** by the deprotection of the triethylsilyl group shows the same helical handedness as in **51**. All of these polymers have a lyotropic liquid crystalline property, while thermotropic liquid crystalline behavior is observed in **50** and **52**. The spin-cast films of **50**–**52** show strong bisignate CD signals centered at the absorption band of the polymer backbone, suggesting the formation of a chiral organization.

An imidazole-functionalized disubstituted acetylene polymer (**53** in Chart 18) has been synthesized *via* a postfunctional strategy<sup>153</sup> and evaluated as a sensor for copper ions and  $\alpha$ -amino acids by fluorescence quenching. Fluorescence quenching is observed at a low Cu<sup>2+</sup> ( $7.0 \times 10^{-7}$  mol L<sup>-1</sup>) concentration. The fluorescence intensity sharply decreases with an increase in Cu<sup>2+</sup> concentration. The addition of  $\alpha$ -amino acids to the solution of the **53**/Cu<sup>2+</sup> complex enhances the fluorescence of **53**, assuming that the  $\alpha$ -amino acid removes copper ions from the complex. Upon addition of glycine, the quenched fluorescence turns on immediately. The detection limit of glycine is as low as  $6.0 \times 10^{-5}$  mol L<sup>-1</sup>.

**3.3.3 Liquid crystalline property.** Polymer **54** is a poly(1-phenyl-1-alkyne) derivative containing a mesogenic pendant with a biphenyl core.<sup>5</sup> It displays a smectic A (SA) mesophase in the temperature range of 172–158 °C when cooled from its isotropic melt. Its cousin (**55**), which has a phenylcyclohexyl core, exhibits a nematic (N) mesophase at much lower temperatures (90–108 °C), although it differs from **54** by only one ring in the mesogenic core (that is, cyclohexyl in **55** *versus* phenyl in **54**).

The liquid crystalline properties and optical anisotropy of poly[1-phenyl-2-*p*-(dimethyl-*n*-octadecylsilylphenyl)acetylene] (**41c**) have been investigated in detail.<sup>154</sup> Polymer **41c** exhibits unexpected smectic phase liquid crystallinity in highly concentrated aromatic organic solvents such as toluene. The two major absorption bands located at 430 and 370 nm are attributable to the  $\pi$ – $\pi^*$  transition parallel to the main chain and the localized  $\pi$ – $\pi^*$  transition with a charge-transfer characteristic among mesogenic repeating units perpendicular to the main chain axis, respectively. Polymer **41c** exhibits highly polarized absorption and fluorescence bands in a sheared film. The main chain axis of the polymer is aligned parallel to the shearing direction, whereas the long axis of the stilbene-like side group is perpendicular to the shearing direction.

A novel acetylene monomer containing a cyanoterphenyl group, namely, 1-[(4'-cyano-4-terphenyl)oxy]-3-octyne, has been polymerized with  $WCl_6$ – $PhSn_4$  catalyst to yield a liquid crystalline aliphatic polyacetylene (**56** in Chart 18).<sup>155</sup> Polymer **56** exhibits a nematic phase according to a polarizing optical microscope and shows a strong emission at 411 nm.

## References

- 1 Review: J. Liu, J. W. Y. Lam and B. Z. Tang, *Chem. Rev.*, 2009, **100**, 1645–1681.
- 2 T. Masuda, F. Sanda and M. Shiotsuki, in *Comprehensive Organometallic Chemistry III*, ed. R. Crabtree and M. Mingos, Elsevier, Oxford, 2007, vol. 11, ch. 16, pp. 557–593.

3 Review: T. Masuda, *J. Polym. Sci., Part A: Polym. Chem.*, 2007, **45**, 165–180.

4 Review: M. G. Mayershofer and O. Nuyken, *J. Polym. Sci., Part A: Polym. Chem.*, 2005, **43**, 5723–5747.

5 Review: J. W. Y. Lam and B. Z. Tang, *Acc. Chem. Res.*, 2005, **38**, 745–754.

6 T. Masuda and F. Sanda, in *Handbook of Metathesis*, ed. R. H. Grubbs, Wiley-VCH, Weinheim, 2003, vol. 3, pp. 375–406.

7 Review: J. Sedlacek and J. Vohlidal, *Collect. Czech. Chem. Commun.*, 2003, **41**, 1745–1790.

8 I. Saeed, M. Shiotsuki and T. Masuda, *Macromolecules*, 2006, **39**, 8977–8981.

9 I. Saeed, M. Shiotsuki and T. Masuda, *Macromolecules*, 2006, **39**, 8567–8573.

10 N. Onishi, M. Shiotsuki, F. Sanda and T. Masuda, *Macromolecules*, 2009, **42**, 4071–4076.

11 T. Nishimura, Y. Ichikawa, T. Hayashi, N. Onishi, M. Shiotsuki and T. Masuda, *Organometallics*, 2009, **28**, 4890–4893.

12 M. Shiotsuki, N. Onishi, F. Sanda and T. Masuda, *Chem. Lett.*, 2010, 244–245.

13 P. Xue, H. S. Y. Sung, I. D. Williams and G. Jia, *J. Organomet. Chem.*, 2006, **691**, 1945–1953.

14 M. V. Jiménez, J. J. Pérez-Torrente, M. I. Bartolomé, E. Vispe, F. J. Lahoz and L. A. Oro, *Macromolecules*, 2009, **42**, 8146–8156.

15 H. Komatsu, Y. Suzuki and H. Yamazaki, *Chem. Lett.*, 2001, 998–999.

16 Y. Kishimoto, T. Miyatake, T. Ikariya and R. Noyori, *Macromolecules*, 1996, **29**, 5054–5055.

17 M. Angoy, M. I. Bartolomé, E. Vispe, P. Lebeda, M. V. Jiménez, J. J. Pérez-Torrente, S. Collins and S. Podzimek, *Macromolecules*, 2010, **43**, 6278–6283.

18 A. L. Gott, P. C. McGowan and C. N. Temple, *Organometallics*, 2008, **28**, 2852–2860.

19 W. Gil, T. Lis, A. Trzeciak and J. J. Ziolkowski, *Inorg. Chim. Acta*, 2006, **359**, 2835–2841.

20 T. Morawitz, S. Bao, M. Bolte, H.-W. Lerner and M. Wagner, *J. Organomet. Chem.*, 2008, **693**, 3878–3884.

21 C. Zhu, N. Yukimura and M. Yamane, *Organometallics*, 2010, **29**, 2098–2013.

22 Y.-H. Wang and F.-Y. Tsai, *Chem. Lett.*, 2007, 1492–1493.

23 S. Abe, K. Hirata, T. Ueno, K. Morino, N. Shimizu, M. Yamamoto, M. Takata, E. Yashima and Y. Watanabe, *J. Am. Chem. Soc.*, 2009, **131**, 6958–6960.

24 M. Kopacka, J. H. Fuhrhop, A. M. Trzeciak, J. J. Ziolkowski and R. Choukroun, *New J. Chem.*, 2008, **32**, 1509–1512.

25 K. H. Park, K. Jang, S. U. Son and D. A. Sweigart, *J. Am. Chem. Soc.*, 2006, **128**, 8740–8741.

26 S. O. Ojwach, I. A. Guzei, J. Darkwa and S. F. Mapolie, *Polyhedron*, 2007, **26**, 851–861.

27 K. Li, M. S. Mohlala, T. V. Segapelo, P. M. Shumbula, I. A. Guzei and J. Darkwa, *Polyhedron*, 2008, **27**, 1017–1023.

28 W. Buchowicz, W. Wojtczak, A. Pietrzykowski, A. Lupa, L. B. Jerzykiewicz, A. Makal and K. Woźniak, *Eur. J. Inorg. Chem.*, 2010, 648–656.

29 T. Katsumata, M. Shiotsuki, F. Sanda, X. Sauvage, L. Delaude and T. Masuda, *Macromol. Chem. Phys.*, 2009, **210**, 1891–1902.

30 P. Csabai, F. Joó, A. M. Trzeciak and J. J. Ziolkowski, *J. Organomet. Chem.*, 2006, **691**, 3371–3376.

31 N. S. Santhosh and G. Sundararajan, *Eur. Polym. J.*, 2007, **43**, 4306–4315.

32 A. Y. Khalimon, R. Simionescu, L. G. Kuzmina, J. A. K. Howard and G. I. Nikonorov, *Angew. Chem., Int. Ed.*, 2008, **47**, 7701–7704.

33 H. Balcar, P. Topka, J. Sedláček, J. Zedník and J. Čejka, *J. Polym. Sci., Part A: Polym. Chem.*, 2008, **46**, 2593–2599.

34 G. Floros, N. Saragas, P. Paraskevopoulou, I. Choinopoulos, S. Koinis, N. Psaroudakis, M. Pitsikalis and K. Metris, *J. Mol. Catal. A: Chem.*, 2008, **289**, 76–81.

35 N. Saragas, G. Floros, P. Paraskevopoulou, N. Psaroudakis, S. Koinis, M. Pitsikalis and K. Metris, *J. Mol. Catal. A: Chem.*, 2009, **303**, 124–131.

36 Review: M. Suginome and Y. Ito, *Adv. Polym. Sci.*, 2004, **171**, 77–136.

37 Review: M. Fujiki, *J. Organomet. Chem.*, 2003, **685**, 15–34.

38 Review: M. Fujiki, J. R. Koe, K. Terao, T. Sato, A. Teramoto and J. Watanabe, *Polym. J. (Tokyo, Jpn.)*, 2003, **35**, 297–344.

39 Review: T. Sato, K. Terao, A. Teramoto and M. Fujiki, *Polymer*, 2003, **44**, 5477–5495.

40 Review: T. Aoki, T. Kaneko and M. Teraguchi, *Polymer*, 2006, **47**, 4867–4892.

41 Review: K. Akagi, *Chem. Rev.*, 2009, **109**, 5354–5401.

42 Review: J. Liu, J. W. Y. Lam and B. Z. Tang, *Chem. Rev.*, 2009, **109**, 5799–5867.

43 Review: E. Yashima, K. Maeda, H. Iida, Y. Furusho and K. Nagai, *Chem. Rev.*, 2009, **109**, 6102–6211.

44 F. Ciardelli, S. Lanzillo and O. Poeroni, *Macromolecules*, 1974, **7**, 174–179.

45 Y. Kishimoto, M. Itou, T. Miyake, T. Ikariya and R. Noyori, *Macromolecules*, 1995, **28**, 6662–6666.

46 A. Furlani, C. Napoletano, M. V. Russo, A. Camus and N. Marsich, *J. Polym. Sci., Part A: Polym. Chem.*, 1989, **27**, 75–86.

47 A. Furlani, C. Napoletano, M. V. Russo and W. J. Feast, *Polym. Bull. (Heidelberg, Ger.)*, 1986, **16**, 311–317.

48 M. Tabata, W. Yang and K. Yokota, *Polym. J. (Tokyo, Jpn.)*, 1990, **22**, 1105–1107.

49 Z. Doležal, R. Kubinec, J. Sedláček, V. Pacáková and J. Vohlidal, *J. Sep. Sci.*, 2007, **30**, 731–739.

50 T. Aoki, T. Kaneko, N. Maruyama, A. Sumi, M. Takahashi, T. Sato and M. Teraguchi, *J. Am. Chem. Soc.*, 2003, **125**, 6346–6347.

51 T. Kaneko, Y. Umeda, T. Yamamoto, M. Teraguchi and T. Aoki, *Macromolecules*, 2005, **38**, 9420–9426.

52 T. Kaneko, Y. Umeda, H. Jia, S. Hadano, M. Teraguchi and T. Aoki, *Macromolecules*, 2007, **40**, 7098–7102.

53 R. Kakuchi, S. Nagata, R. Sakai, I. Otsuka, H. Nakade, T. Satoh and T. Kakuchi, *Chem.–Eur. J.*, 2008, **14**, 10259–10266.

54 R. Kakuchi, T. Kodama, R. Shimada, Y. Tago, R. Sakai, T. Satoh and T. Kakuchi, *Macromolecules*, 2009, **42**, 3892–3897.

55 K. K. L. Cheuk, B. S. Li, J. W. Y. Lam, Y. Xie and B. Z. Tang, *Macromolecules*, 2008, **41**, 5997–6005.

56 K. Terada, T. Masuda and F. Sanda, *J. Polym. Sci., Part A: Polym. Chem.*, 2009, **47**, 4971–4981.

57 T. Fukushima, K. Takachi and K. Tsuchihara, *Macromolecules*, 2006, **39**, 3103–3105.

58 T. Fukushima, H. Kimura and K. Tsuchihara, *Macromolecules*, 2009, **42**, 8619–8626.

59 J. Qu, R. Kawasaki, M. Shiotsuki, F. Sanda and T. Masuda, *Polymer*, 2006, **47**, 6551–6559.

60 K. Tamura, T. Fujii, M. Shiotsuki, F. Sanda and T. Masuda, *Polymer*, 2008, **49**, 4494–4501.

61 H.-P. Xu, B.-Y. Xie, W.-Z. Yuan, J.-Z. Sun, F. Yang, Y.-Q. Dong, A. Qin, S. Zhang, M. Wang and B. Z. Tang, *Chem. Commun.*, 2007, 1322–1324.

62 A. Miyasaka, T. Sone, Y. Mawatari, S. Setayesh, K. Müllen and M. Tabata, *Macromol. Chem. Phys.*, 2006, **207**, 1938–1944.

63 H. Zhao, W. Z. Yuan, J. Mei, L. Tang, X. Q. Liu, J. M. Yan, X. Y. Shen, J. Z. Sun, A. Qin and B. Z. Tang, *J. Polym. Sci., Part A: Polym. Chem.*, 2009, **47**, 4995–5005.

64 W. Z. Yuan, J. Z. Sun, Y. Dong, M. Halussler, F. Yang, H. P. Xu, A. Qin, J. W. Y. Lam, Q. Zheng and B. Z. Tang, *Macromolecules*, 2006, **39**, 8011–8020.

65 W. Z. Yuan, J. Z. Sun, J. Z. Liu, Y. Dong, Z. Li, H. P. Xu, A. Qin, M. Hussler, J. K. Jin, Q. Zheng and B. Z. Tang, *J. Phys. Chem. B*, 2008, **112**, 8896–8905.

66 T. Fulghum, S. M. Abdul Karim, A. Baba, P. Taranekar, T. Nakai, T. Masuda and R. C. Advincula, *Macromolecules*, 2006, **39**, 1467–1473.

67 H. Murata, D. Miyajima and H. Nishide, *Macromolecules*, 2006, **39**, 6331–6335.

68 J. Qu, T. Katsumata, M. Satoh, J. Wada, J. Igarashi, K. Mizoguchi and T. Masuda, *Chem.–Eur. J.*, 2007, **13**, 7965–7973.

69 J. G. Rodríguez and J. L. Tejedor, *J. Polym. Sci., Part A: Polym. Chem.*, 2007, **45**, 2038–2047.

70 J. M. Reyna-González, M. Aguilar-Martínez, A. García-Concha, C. Palomar and E. Rivera, *Synth. Met.*, 2009, **159**, 659–665.

71 F. Sanda, R. Kawasaki, M. Shiotsuki and T. Masuda, *J. Polym. Sci., Part A: Polym. Chem.*, 2007, **45**, 4450–4458.

72 J. Qu, R. Kawasaki, M. Shiotsuki, F. Sanda and T. Masuda, *Polymer*, 2007, **48**, 467–476.

73 F. Sanda, R. Kawasaki, M. Shiotsuki, T. Takashima, A. Fujii, M. Ozaki and T. Masuda, *Macromol. Chem. Phys.*, 2007, **208**, 765–771.

74 R. Nomura, J. Tabei and T. Masuda, *J. Am. Chem. Soc.*, 2001, **123**, 8430–8431.

75 F. Sanda, T. Fujii, J. Tabei, M. Shiotsuki and T. Masuda, *Macromol. Chem. Phys.*, 2008, **209**, 112–118.

76 F. Sanda, T. Fujii, M. Shiotsuki and T. Masuda, *Polym. J. (Tokyo, Jpn.)*, 2008, **40**, 768–774.

77 T. Fujii, M. Shiotsuki, Y. Inai, F. Sanda and T. Masuda, *Macromolecules*, 2007, **40**, 7079–7088.

78 F. Sanda and T. Endo, *Macromol. Chem. Phys.*, 1999, **200**, 2651–2661.

79 H. Zhao, F. Sanda and T. Masuda, *Macromolecules*, 2004, **37**, 8888–8892.

80 H. Zhao, F. Sanda and T. Masuda, *Polymer*, 2006, **47**, 2596–2602.

81 H. Zhao, F. Sanda and T. Masuda, *J. Polym. Sci., Part A: Polym. Chem.*, 2007, **45**, 253–261.

82 F. Sanda, K. Terada and T. Masuda, *Macromolecules*, 2005, **38**, 8149–8154.

83 H. Zhao, F. Sanda and T. Masuda, *Macromolecules*, 2004, **37**, 8893–8896.

84 H. Zhao, F. Sanda and T. Masuda, *Polymer*, 2006, **47**, 1584–1589.

85 R. Liu, F. Sanda and T. Masuda, *Polymer*, 2007, **48**, 6510–6518.

86 R. Liu, F. Sanda and T. Masuda, *J. Polym. Sci., Part A: Polym. Chem.*, 2008, **46**, 4175–4182.

87 J. Kadokawa, K. Tawa, M. Suenaga, Y. Kaneko and M. Tabata, *J. Macromol. Sci., Part A: Pure Appl. Chem.*, 2006, **43**, 1179–1187.

88 M. Suenaga, Y. Kaneko, J. Kadokawa, T. Nishikawa, H. Mori and M. Tabata, *Macromol. Biosci.*, 2006, **6**, 1009–1018.

89 Y. Sasaki, Y. Kaneko and J. Kadokawa, *Polym. Bull. (Heidelberg, Ger.)*, 2009, **62**, 291–303.

90 J. Deng, B. Chen, X. Luo and W. Yang, *Macromolecules*, 2009, **42**, 933–938.

91 B. Chen, J. Deng, X. Liu and W. Yang, *Macromolecules*, 2010, **43**, 3177–3182.

92 X. Luo, L. Li, J. Deng, T. Guo and W. Yang, *Chem. Commun.*, 2010, **46**, 2745–2747.

93 D. Yue, T. Fujii, K. Terada, J. Tabei, M. Shiotsuki, F. Sanda and T. Masuda, *Macromol. Rapid Commun.*, 2006, **27**, 1460–1464.

94 D. Yue, M. Shiotsuki, F. Sanda and T. Masuda, *Polymer*, 2007, **48**, 68–73.

95 D. Yue, T. Fujii, K. Terada, J. Tabei, M. Shiotsuki, F. Sanda and T. Masuda, *J. Polym. Sci., Part A: Polym. Chem.*, 2007, **45**, 1515–1524.

96 M. Yang, M. Zheng, A. Furlani and M. V. Russo, *J. Polym. Sci., Part A: Polym. Chem.*, 1994, **32**, 2709–2713.

97 A. Furlani, M. V. Russo and A. Longo, *Polymer*, 1997, **38**, 183–189.

98 M. V. Russo, A. Furlani, P. Altamura and I. Fratoddi, *Polymer*, 1997, **38**, 3677–3690.

99 X. Zhan, M. Yang and H. Sun, *Catal. Lett.*, 2000, **70**, 79–82.

100 X. Zhan, M. Yang and H. Sun, *Macromol. Rapid Commun.*, 2001, **22**, 530–534.

101 Z. Lu and S. Ma, *J. Org. Chem.*, 2006, **71**, 2655–2660.

102 S. S. Palimkar, P. H. Kumer, R. J. Lahoti and K. V. Srinivasan, *Tetrahedron*, 2006, **62**, 5109–5115.

103 J. M. Marshall, P. Eidam and H. S. Eidam, *J. Org. Chem.*, 2006, **71**, 4840–4844.

104 L. B. Han, Y. Ono and H. Yazawa, *Org. Lett.*, 2005, **7**, 2909–2911.

105 Y. Suzuki, M. Shiotsuki, F. Sanda and T. Masuda, *Macromolecules*, 2007, **40**, 1864–1867.

106 Y. Suzuki, M. Shiotsuki, F. Sanda and T. Masuda, *Chem.-Asian J.*, 2008, **3**, 2075–2081.

107 J. Qu, M. Shiotsuki, F. Sanda and T. Masuda, *Macromol. Chem. Phys.*, 2007, **208**, 823–832.

108 J. Qu, Y. Suzuki, M. Shiotsuki, F. Sanda and T. Masuda, *Macromol. Chem. Phys.*, 2007, **208**, 1992–1999.

109 J. Qu, Y. Suzuki, M. Shiotsuki, F. Sanda and T. Masuda, *Polymer*, 2007, **48**, 4628–4636.

110 J. Qu, Y. Suzuki, M. Shiotsuki, F. Sanda and T. Masuda, *Polymer*, 2007, **48**, 6491–6500.

111 J. Qu, F. Jiang, H. Chen, F. Sanda and T. Masuda, *J. Polym. Sci., Part A: Polym. Chem.*, 2009, **47**, 4749–4761.

112 J. Qu, F. Sanda and T. Masuda, *Eur. Polym. J.*, 2009, **45**, 448–454.

113 M. Shiotsuki, W. Zhang and T. Masuda, *Polym. J. (Tokyo, Jpn.)*, 2007, **39**, 690–695.

114 W. Zhang, M. Shiotsuki and T. Masuda, *Macromol. Rapid Commun.*, 2007, **28**, 1115–1121.

115 Y. Shirakawa, Y. Suzuki, K. Terada, M. Shiotsuki, T. Masuda and F. Sanda, *Macromolecules*, 2010, **43**, 5575–5581.

116 Z. Qin, Y. Chen, W. Zhou, X. He, F. Bai and M. Wan, *Eur. Polym. J.*, 2008, **44**, 3732–3740.

117 K. Nagai, Y. M. Lee and T. Masuda, in *Macromolecular Engineering*, ed. K. Matyjaszewsky, Y. Gnanou and L. Leibler, Wiley-VCH, Weinheim, Germany, 2007, part 4, ch. 19.

118 T. Masuda and K. Nagai, in *Materials Science of Membranes*, ed. Y. Yampolskii, I. Pinnau and B. D. Freeman, Wiley, Chichester, UK, 2006, ch. 8.

119 Review: M. Ulbricht, *Polymer*, 2006, **47**, 2217–2262.

120 Review: K. Nagai, T. Masuda, T. Nakagawa, B. D. Freeman and I. Pinnau, *Prog. Polym. Sci.*, 2001, **26**, 721–798.

121 L. M. Robeson, W. F. Burgoyne, M. Langsam, A. C. Savoca and C. F. Tien, *Polymer*, 1994, **35**, 4970–4978.

122 G. Kwak and T. Masuda, *J. Polym. Sci., Part A: Polym. Chem.*, 2000, **38**, 2964–2969.

123 T. Sakaguchi, K. Yamoto, M. Shiotsuki, F. Sanda, M. Yoshikawa and T. Masuda, *Macromolecules*, 2005, **38**, 2704–2709.

124 T. Sakaguchi, M. Shiotsuki, F. Sanda, B. D. Freeman and T. Masuda, *Macromolecules*, 2005, **38**, 8327–8332.

125 Y. Shida, T. Sakaguchi, M. Shiotsuki, F. Sanda, B. D. Freeman and T. Masuda, *Macromolecules*, 2005, **38**, 4096–4102.

126 Y. Hu, T. Shimizu, K. Hattori, M. Shiotsuki, F. Sanda and T. Masuda, *J. Polym. Sci., Part A: Polym. Chem.*, 2010, **48**, 861–868.

127 A. Fukui, K. Hattori, Y. Hu, M. Shiotsuki, F. Sanda and T. Masuda, *Polymer*, 2009, **50**, 4159–4165.

128 Y. Hu, M. Shiotsuki, F. Sanda, B. D. Freeman and T. Masuda, *Macromolecules*, 2008, **41**, 8525–8532.

129 A. V. Volkov, V. V. Volkov and V. S. Khotimskii, *Vysokomol. Soedin., Ser. A Ser. B*, 2009, **51**, 2113–2128.

130 Yu. V. Kostina, A. B. Gil'man, A. V. Volkov, M. S. Piskarev, S. A. Legkov, E. G. Litvinova, V. S. Khotimskii and G. N. Bondarenko, *High Energy Chem.*, 2009, **43**, 509–511.

131 L. Shao, J. Samseth and M.-B. Haegg, *J. Appl. Polym. Sci.*, 2009, **113**, 3078–3088.

132 S. D. Kelman, B. W. Rowe, C. W. Bielawski, S. J. Pas, A. J. Hill, D. R. Paul and B. D. Freeman, *J. Membr. Sci.*, 2008, **320**, 123–134.

133 S. Matteucci, V. A. Kusuma, S. D. Kelman and B. D. Freeman, *Polymer*, 2008, **49**, 1659–1675.

134 A. A. Masalev, V. S. Khotimskii, G. N. Bondarenko and M. V. Chirkova, *Vysokomol. Soedin., Ser. A Ser. B*, 2008, **50**, 47–53.

135 R. D. Raharjo, B. D. Freeman, D. R. Paul and E. S. Sanders, *Polymer*, 2007, **48**, 7329–7344.

136 J. Qiu, M. Zheng and K. V. Peinemann, *Macromolecules*, 2007, **40**, 3213–3222.

137 V. L. Khodzhaeva and V. G. Zaikin, *J. Appl. Polym. Sci.*, 2007, **103**, 2523–2527.

138 P. Winberg, K. DeSitter, C. Dotremont, S. Mullens, I. F. J. Vankelecom and F. H. J. Maurer, *Macromolecules*, 2005, **38**, 3776–3782.

139 R. D. Raharjo, H. J. Lee, B. D. Freeman, T. Sakaguchi and T. Masuda, *Polymer*, 2005, **46**, 6316–6324.

140 A. Takeda, T. Sakaguchi and T. Hashimoto, *Polymer*, 2009, **50**, 5031–5036.

141 H. Ito, E. Akiyama, H. Yokota and K. Takedai, *US Pat., Appl. Publ.*, 2007, 20070231654.

142 T. Sakaguchi, K. Kameoka and T. Hashimoto, *J. Polym. Sci., Part A: Polym. Chem.*, 2009, **47**, 6463–6471.

143 G. Kwak, H.-Q. Wang, K.-H. Choi, K.-H. Song, S.-H. Kim, H.-S. Kim, S.-J. Lee, H.-Y. Cho, E.-J. Yu, H.-J. Lee, E.-J. Park and L.-S. Park, *Macromol. Rapid Commun.*, 2007, **28**, 1317–1324.

144 G. Kwak, M. Minakuchi, T. Sakaguchi, T. Masuda and M. Fujiki, *Macromolecules*, 2008, **41**, 2743–2746.

145 J. Chen, H. S. Kwok and B. Z. Tang, *J. Polym. Sci., Part A: Polym. Chem.*, 2006, **44**, 2487–2498.

146 C. C. W. Law, J. W. Y. Lam, A. Qin, Y. Dong, H. S. Kwok and B. Z. Tang, *Polymer*, 2006, **47**, 6642–6651.

147 C. Huang, S. Yang, K. Chen and C. Hsu, *J. Polym. Sci., Part A: Polym. Chem.*, 2006, **44**, 519–531.

148 C.-H. Huang, C.-W. Lee, C.-S. Hsu, C. Renaud and T.-P. Nguyen, *Thin Solid Films*, 2007, **515**, 7671–7674.

149 S.-H. Yang, C.-H. Huang, C.-H. Chen and C.-S. Hsu, *Macromol. Chem. Phys.*, 2009, **210**, 37–47.

150 H. Xu, J. Sun, A. Qin, J. Hua, Z. Li, Y. Dong, H. Xu, W. Yuan, Y. Ma, M. Wang and B. Z. Tang, *J. Phys. Chem. B*, 2006, **110**, 21701–21709.

151 M. Teraguchi, J. Suzuki, T. Kaneko, T. Aoki and T. Masuda, *Macromolecules*, 2003, **36**, 9694–9697.

152 T. Fukushima and K. Tsuchihara, *Macromolecules*, 2009, **42**, 5453–5460.

153 Q. Zeng, C. K. W. Jim, J. W. Y. Lam, Y. Dong, Z. Li, J. Qin and B. Z. Tang, *Macromol. Rapid Commun.*, 2009, **30**, 170–175.

154 G. Kwak, M. Minakuchi, T. Sakaguchi, T. Masuda and M. Fujiki, *Chem. Mater.*, 2007, **19**, 3654–3661.

155 L. Chen, Y. Chen, W. Zhou and X. He, *Synth. Met.*, 2009, **159**, 576–582.